Journal of Neurochemistry, 2006, **97**, 488–503 doi:10.1111/j.1471-4159.2006.03766.x

Cortical choline transporter function measured *in vivo* using choline-sensitive microelectrodes: clearance of endogenous and exogenous choline and effects of removal of cholinergic terminals

V. Parikh and M. Sarter

Department of Psychology, University of Michigan, Ann Arbor, Michigan, USA

Abstract

The capacity of the high-affinity choline transporter (CHT) to import choline into presynaptic terminals is essential for acetylcholine synthesis. Ceramic-based microelectrodes, coated at recording sites with choline oxidase to detect extracellular choline concentration changes, were attached to multibarrel glass micropipettes and implanted into the rat frontoparietal cortex. Pressure ejections of hemicholinium-3 (HC-3), a selective CHT blocker, dose-dependently reduced the uptake rate of exogenous choline as well as that of choline generated in response to terminal depolarization. Following the removal of CHTs, choline signal recordings confirmed that the demonstration of potassium-induced choline signals and HC-3-induced decreases in choline clearance require the presence of cholinergic terminals. The results obtained from lesioned animals also confirmed the selectivity of the effects of HC-3 on choline clearance in intact animals. Residual cortical choline clearance correlated significantly with CHT-immunoreactivity in lesioned and intact animals. Finally, synaptosomal choline uptake assays were conducted under conditions reflecting *in vivo* basal extracellular choline concentrations. Results from these assays confirmed the capacity of CHTs measured *in vivo* and indicated that diffusion of substrate away from the electrode did not confound the *in vivo* findings. Collectively, these results indicate that increases in extracellular choline concentrations, irrespective of source, are rapidly cleared by CHTs.

Keywords: acetylcholine, choline, choline-sensitive microelectrodes, choline transporter, choline uptake, hemicholinium-3.

J. Neurochem. (2006) **97**, 488–503.

The cortical mantle receives a dense cholinergic projection originating from the nucleus basalis of Meynert (nBM) and the substantia innominata (SI) in the basal forebrain (BF). The cortical cholinergic input system represents a major component of the attention systems of the brain; abnormalities in cholinergic neurotransmission have been hypothesized to contribute to the symptoms of major cognitive disorders (Everitt and Robbins 1997; Zaborszky 2002; Hasselmo and McGaughy 2004; Mesulam 2004; Sarter *et al*. 2005a,b). The transport of choline into presynaptic terminals, via a Na^+/Cl^--dependent, hemicholinium-3 (HC-3)-sensitive choline transporter (CHT), is the rate-limiting step of acetylcholine (ACh) synthesis (Yamamura and Snyder 1972; Guyenet *et al*. 1973; Atweh *et al*. 1975; Simon and Kuhar 1975, 1976; Simon *et al*. 1976; Blusztajn and Wurtman 1983; Chatterjee *et al*. 1987; Saltarelli *et al*. 1987; Lockman and Allen 2002). HC-3-induced blockade of the CHT is sufficient to attenuate ACh synthesis and release (Freeman *et al*. 1979; Saltarelli *et al*. 1987).

Rapid and robust changes in the capacity of the CHT to transport choline have been demonstrated as a result of either molecular or behavioral/cognitive manipulations (Brandon *et al*. 2004; Ferguson *et al*. 2004; Apparsundaram *et al*. 2005). Such changes in CHT capacity appear to be caused in part by altered trafficking of CHTs between intracellular

Received November 22, 2005; revised manuscript received December 29, 2005; accepted January 3, 2006.

Address correspondence and reprint requests to Martin Sarter, Department of Psychology, University of Michigan, 530 Church Street, Ann Arbor, MI 48109–1043, USA. E-mail: msarter@umich.edu

Abbreviations used: AA, ascorbic acid; ACh, acetylcholine; AChE, acetylcholine esterase; BF, basal forebrain; BSA, bovine serum albumin; CHT, choline transporter; CO, choline oxidase; DA, dopamine; DAB, 3′,3′-diaminobenzidine dihydrochloride; FBNF1, Fisher/Brown Norway hybrid rats; HC-3, hemicholinium-3; IR, immunoreactivity; KBB, Kreb's bicarbonate buffer; LOD, limit of detection; LSD, least significant difference; Ms-SAP, mouse-IgG saporin; nBM, nucleus basalis of Meynert; PBS, phosphate-buffered saline; R^2, linearity; SI, substantia innominata; 192-SAP, 192-IgG saporin; TBS, Tris-buffered saline.

domains and the plasma membrane (Ferguson *et al*. 2003; Ferguson and Blakely 2004; Apparsundaram *et al*. 2005). Several intracellular signaling molecules have been shown to be involved in the regulation of both CHT surface expression and CHT capacity (Saltarelli *et al*. 1990; Gates *et al*. 2004), suggesting that the capacity of the CHT is regulated by multiple cholinergic and possibly non-cholinergic mechanisms. Abnormally regulated CHTs have been hypothesized to contribute to cognitive impairments (Wurtman 1992; Slotkin *et al*. 1994; Sarter and Parikh 2005).

Previous studies determined the properties of CHTs primarily on the basis of *in vitro* choline uptake assays. Data from such assays substantiated the high affinity of CHTs for choline (K_m = 1–10 μM; Haga 1971; Farber *et al*. 1996; Lockman and Allen 2002) and suggested a considerable range of CHT-saturating choline concentrations (5–30 μM). Furthermore, a close relationship between cholinergic neuronal activity and CHT capacity was demonstrated (Atweh *et al*. 1975; Simon and Kuhar 1975; Simon *et al*. 1976).

Using choline-sensitive microelectrodes and an amperometric method for the measurement of extracellular choline concentrations *in vivo* (Burmeister and Gerhardt 2001; Burmeister *et al*. 2003; Parikh *et al*. 2004), the present experiments were designed to determine the contribution of the CHT to the clearance of exogenous choline as well as choline derived from newly released ACh in the rat cortex. The experimental approaches employed to address these issues here correspond with those used by Gerhardt and colleagues for the study of dopamine clearance via dopamine transporters (Cass *et al*. 1993). Choline clearance was determined in either the presence or the absence of a highly potent and selective inhibitor of CHTs, HC-3 (Guyenet *et al*. 1973; Simon and Kuhar 1975), in intact animals and following the removal of cholinergic terminals in the recording region. *In vitro* synaptosomal assays were conducted under conditions that mimicked extracellular choline concentrations determined *in vivo*, in order to verify the contribution of CHTs to choline clearance determined *in vivo*. The results provide quantitative insights into the contribution of CHTs *in vivo* to the clearance of choline hydrolyzed from local increases in ACh release as well as that of exogenous choline.

Materials and methods

Subjects

Adult male Fisher/Brown Norway hybrid rats (FBNF1; Harlan, Indianapolis, IN, USA), weighing 200–250 g at the beginning of the experiments were used. Animals were individually housed in a temperature- (23°C) and humidity-controlled (45%) environment and on a 12 h light/dark cycle (lights on at 06:30 h). Animals were extensively handled prior to the beginning of experiments to minimize potential confounds resulting from the effects of either novelty or stress. Food and water were made available *ad libitum* (Rodent Chow; Harlan Teklad, Madison, WI, USA). All procedures were conducted in adherence with protocols approved by the University Committee on Use and Care of Animals (UCUCA).

Drugs and chemicals

Choline oxidase (CO; EC 1.1.3.17), bovine serum albumin (BSA), glutaraldehyde, ascorbic acid (AA), dopamine (DA), choline, hemicholinium-3 (HC-3), acetylthiocholine iodide and 3′,3′-diaminobenzidine dihydrochloride (DAB) were all obtained from Sigma Chemical Co. (St Louis, MO, USA). Nafion™ (5% in a mixture of aliphatic alcohols and water) was obtained from Aldrich Chemical Co. (Milwaukee, WI, USA). 192-IgG Saporin (192-SAP) and mouse-IgG saporin (Ms-SAP) were obtained from Advanced Targeting Systems (San Diego, CA, USA). Rabbit anti-choline transporter (CHT) polyclonal antibody and goat serum was from Chemicon (Chemicon International, Temecula, CA, USA). Alexa Fluor® 488-conjugated goat anti-rabbit IgG (highly cross-adsorbed) and Prolong-Gold anti-fade reagent were obtained from Molecular Probes (Eugene, OR, USA). [*Methyl*-^{3}H]Choline chloride was purchased from Amersham Biosciences Inc. (Piscataway, NJ, USA). HPLC grade water (Fisher Scientific, Davis, CA, USA) was used to prepare all solutions. Solutions used for intracranial injections were prepared in 0.9% NaCl (pH 7.4) and filtered through 0.22-μm sterile non-pyrogenic filters (Costar, Corning, NY, USA) prior to use.

Lesion surgery

All surgeries were performed under aseptic conditions. Anesthesia was induced with 4–5% isoflurane using an anesthesia machine (Anesco/Surgivet, Waukesha, WI, USA). Rats were placed in a stereotaxic instrument (model No. 962; David Kopf, Tujunga, CA, USA) and anesthesia was maintained with 2% isoflurane along with oxygen at a flow rate of 1 mL/min. Loss of cortical cholinergic inputs was produced by infusions of 192-SAP into the region of the cholinergic cell bodies in the nucleus basalis of Meynert and substantia innominata of the BF. The selective cholinotoxic effects of 192-SAP, a conjugate of an antibody to the p75 neurotrophin receptor and the ribosome-deactivating protein saporin, has been extensively documented (e.g. Book *et al*. 1992; Holley *et al*. 1994; Waite *et al*. 1994). Animals (n = 10) received bilateral infusions of 192-SAP (0.085 μg/0.5 μL/hemisphere) into BF using the following coordinates [anterior-posterior, −1.3 mm; medial-lateral, ±2.5 mm (relative to bregma); dorsal-ventral, −7.2 mm (relative to dura); Paxinos and Watson 1988]. Sham lesions were produced by infusing Ms-SAP (0.1 μg/0.5 μL/hemisphere), a conjugate of pre-immune mouse IgG antibody and saporin, into BF. Infusions were made at a rate of 0.25 μL/min using a 1-μL Hamilton microsyringe; the needle remained in place for an additional 4 min following the infusion. Amperometric recording sessions (see below) were performed three weeks after lesion surgeries.

Preparation and calibration of choline-sensitive microelectrodes

Choline-sensitive microelectrodes were prepared using ceramic-based, multisite microelectrodes featuring four 15 × 333 μm platinum recording sites arranged in side-by-side pairs (see Fig. 1a; Burmeister *et al*. 2003; Parikh *et al*. 2004). Briefly, the selectivity of the microelectrode for choline was enhanced by applying Nafion™

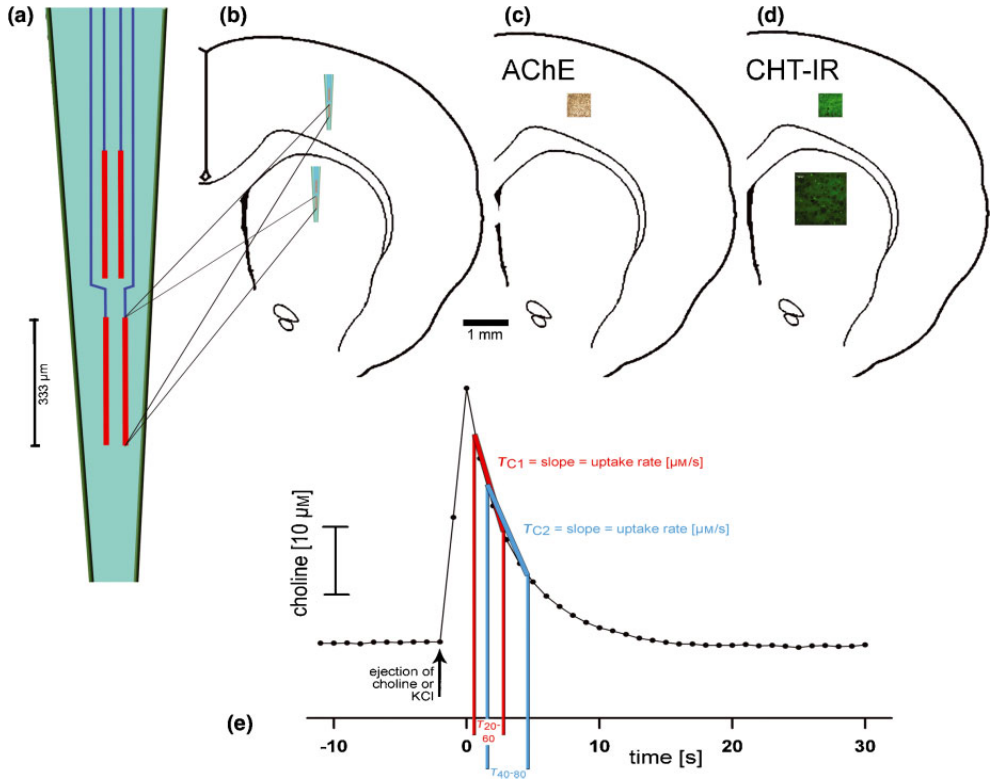

Fig. 1 Arrangements and dimensions of the four recording areas on the ceramic-based microelectrodes. Individual recording sites were 333 × 15 µm (see scale for recording site length on the right). The lower pair of recording sites was typically coated with choline oxidase while the upper pair was used for self-referencing. (b) placement of the recording sites in the frontoparietal cortex and striatum (the 1 mm scale applies to the schematics b–d). (c) and (d) depict the location and dimensions of the sampling areas for quantification of AChE-positive fiber density and CHT-IR in the frontoparietal cortex and striatum. (e) illustration of the main parameters used to quantify choline signals, specifically, choline clearance *in vivo*. Pilot data indicated that a later phase of the clearance function, bordered by a 40% and 80% decrease in choline concentration relative to peak amplitude, is more sensitive to the effects of HC-3 than an earlier phase which is bordered by a 20% to 60% decrease in choline concentration. Based on this observation, and using a modified terminology to describe and quantify transporter-mediated clearance (see Methods for references), and in addition to signal amplitude, the uptake rates of an early (T_{C1}) and a later (T_{C2}) component of the choline clearance function were determined in (µM/s). Furthermore, the times (s) required for the signal to decline between 20% and 60% ($T_{20–60}$) and 40% and 80% ($T_{40–80}$), relative to the maximal amplitude, were calculated (in ms).

coatings prior to enzyme application. Nafion is a charged polymer that limits the access of potentially interfering analytes to the recording surface; in contrast, the electrode remains permeable for H_2O_2, the reporter molecule indicating choline oxidation. CO was cross-linked with the BSA-glutaraldehyde mixture and immobilized on the two lower recording sites. The upper two recording sites were coated only with the BSA-glutaraldehyde solution and served to record background activity. Enzyme-coated microelectrodes were air dried at least 48–72 h prior to use. Choline-sensitive microelectrodes were calibrated using a FAST-16 electrochemical recording system (LLC; Quanteon, Nicholasville, KY, USA) prior to implantation in animals. Microelectrodes were dipped in 0.05 M phosphate-buffered saline (PBS) for 30 min prior to calibration. Calibrations were performed using fixed potential amperometry by applying a constant voltage of 0.7 V versus an Ag/AgCl reference electrode (Bioanalytical Systems Inc., West Lafayette, IN, USA) in a beaker containing a stirred solution of 0.05 M PBS maintained at 37°C. Amperometric currents were digitized at a frequency of 5 Hz. After achieving a stable baseline current, aliquots of stock solutions of AA (20 mM), choline (20 mM) and DA (2 mM) were added to the calibration beaker such that the final concentrations were 250 µM AA, 20, 40, 60 and 80 µM choline and 2 µM DA. Normalized currents recorded from non-CO-coated sites were subtracted from normalized currents recorded via CO-coated sites ('self-referencing') to yield currents that selectively reflected choline concentrations (Burmeister and Gerhardt 2001; Parikh *et al*. 2004). The slope (sensitivity), limit of detection (LOD) and linearity (R^2) for choline, as well as selectivity ratio for AA and DA, were calculated in individual channels as well as in self-referencing mode. To be used in subsequent *in vivo* experiments, electrodes were required to meet the following characteristics: sensitivity for detecting choline, >3 pA/µM, with a background current of <100 pA; LOD < 300 nM choline; selectivity for choline : AA, >80 : 1; detection of increasing choline concentrations (20–80 µM), $R^2 > 0.98$.

In vivo recordings

Recordings were carried out in frontoparietal cortex of rats anesthetized with urethane (1.25–1.5 g/kg, i.p.; see Fig. 1b for an illustration of the electrode placement). Animals were placed in a stereotaxic frame and their body temperatures were maintained at 37°C using a Deltaphase isothermal pad (Braintree Scientific, Braintree, MA, USA). Triple-barrel glass capillaries (1.2 mm × 0.60 mm, 6 in; A-M systems, Inc., Carlsborg, WA, USA) were pulled using a micropipette puller (model No. 51210; Stoelting, Wood Dale, IL, USA) and then bumped against a glass slide until the inner tip diameter of an individual barrel was ~15–20 μm. The micropipette was attached to the microelectrode using sticky wax such that the tip of the micropipette was placed between the lower and upper pairs of recordings sites, and the distance between the tip and the microelectrode was 70–100 μm. An Ag/AgCl reference electrode prepared from 200 μm diameter silver wire (A-M Systems) and was implanted at a site remote to the recording area. The individual barrels of the micropipette were filled with drug solution (see below) prior to microelectrode implantation. The microelectrode/micropipette assembly was slowly lowered into the frontoparietal cortex (AP, +1.0 mm; ML, ±2.7 mm; DV, −1.0 mm; measured from bregma), using a microdrive (MO-10; Narishige International, East Meadow, NY, USA). Drug solutions were ejected from the micropipettes using PTFE tubing connected to a pressure ejection system (Picospritzer III; Parker Hannifin Co., Fairfield, NJ, USA) at 2–10 psi for 1–2 s. The ejected volumes were monitored using a stereomicroscope (Meiji Techno America, San Jose, CA, USA) fitted with a reticule. Amperometric recordings were made every 100 ms by applying a fixed potential of 0.7 V to the microelectrode using the FAST-16 recording system (Quanteon). Data were digitized using FAST-16 software. Experiments began following the stabilization of the baseline current for 30–45 min. To determine, *in vivo*, the contribution of the CHT to the rapid clearance of exogenous choline, the effects of HC-3, a potent and selective CHT blocker (Guyenet *et al*. 1973; Manaker *et al*. 1986), were evaluated. In sham-lesioned controls ($n = 8$) and 192-SAP-lesioned rats ($n = 10$), the effects of local ejections of 5 mM choline (100–300 nL) were assessed in the presence and absence of HC-3 (1 and 10 μM). In each animal, the effects of 3–5 ejections per condition were tested. In addition, the effects of pressure ejections of 200 nL KCl (70 mM; Parikh *et al*. 2004) in sham- and 192-SAP-lesioned rats served to demonstrate the effects of loss of cholinergic terminals on depolarization-evoked choline signals. Tests of the effects of KCl and exogenous choline were separated by 10–15 min to ensure stable baseline activity. The volumes of either choline or choline + HC-3 pressure ejections were varied by adjusting the pressure in order to obtain choline signals with uniform amplitudes (20–25 μM). Uniform amplitudes are a prerequisite for valid comparisons between the effects of different manipulations on choline uptake rate, and they limit the variations based on clearance via the substrate-regulated low-affinity choline transporter (Parikh *et al*. 2004). The effects of potassium ejections (70 mM), in combination with HC-3 (1 and 10 μM), served to determine HC-3-sensitive clearance of choline that is derived from terminal depolarization and hydrolysis of newly released ACh; these experiments were carried out in a separate set of animals ($n = 5$). Previous experiments demonstrated that KCl-induced choline signals are attenuated by the administration of either an acetylcholine esterase (AChE) inhibitor or tetrodotoxin (Parikh *et al*. 2004). Although we planned to adjust the volume of pressure ejections of KCl individually (150–200 nL) in order to obtain uniform signal amplitudes (10–15 μM) across animals, this was not necessary (see Discussion). To control for the specificity of the effects of the lesions (below), KCl-induced signals were also recorded in the dorsal striatum (see Fig. 1b).

Choline signal analysis

For self-referencing, normalized signals recorded via the non-CO-coated channel were subtracted from normalized signals obtained at the CO-coated channel (Burmeister and Gerhardt 2001). Self-referencing was applied for the analyses of choline signals associated with relatively high background noise (>3 μM), and if pressure ejection artifacts were observed on the CO-coated channel.

Five parameters were derived from choline signals and subjected to statistical analysis: the ratio between the signal amplitude and the ejection volume (nM of equivalent choline per nL of solution), time (s) required for the signal to decline between 20 and 60% of the maximal amplitude (T_{20-60}) and between 40 and 80% of the maximal amplitude (T_{40-80}), and the choline uptake rate (μM/s) for the earlier (T_{C1}) and later (T_{C2}) part of the choline clearance function (see Fig. 1e). T_{C1} and T_{C2} were obtained by determining the slope of the linear regression of data points from the respective part of the clearance curve. These parameters were selected on the basis of findings from studies on the clearance of dopamine and serotonin, including the effects of uptake inhibitors on the clearance of these transmitters (Wightman *et al*. 1988; Friedemann and Gerhardt 1992; Cass *et al*. 1993; Daws *et al*. 1997; Zahniser *et al*. 1999). Generally, T_{C1} and T_{20-60} have been suggested to represent the slope of the initial linear portion of signal clearance (T_{20-60}), and to reflect the capacity of DA transporters (Wightman *et al*. 1988; Zahniser *et al*. 1999). However, pilot data indicated that the effects of HC-3 on choline clearance manifest more robustly with respect to an overlapping but later component of the clearance curve (T_{C2}, T_{40-80}). Thus, both components of the clearance curve were analyzed (see Fig. 1e for a graphical illustration of these parameters). The average of three responses per manipulation per animal were used for statistical analyses of clearance data.

Determination of basal extracellular choline concentration

Basal extracellular choline levels were determined in frontoparietal cortex from CO-coated recording sites by subtracting the *in vivo* background current exhibited by these channels from non-CO-coated channels and dividing the difference by the sensitivity (calibration slope) of the enzyme-coated channel. The valid determination of basal extracellular choline levels *in vivo* required the use of microelectrodes with the following electrochemical characteristics: (i) identical background currents on both enzyme-coated and non-enzyme-coated channels (difference <10 pA) prior to any analyte addition during calibration; (ii) CO-coated and non-CO-coated cannels were relatively insensitive to AA as indicated by a <5 pA change in current in response to the addition of 500 μL of 20 mM AA.

Histochemical and immunohistochemical procedures

After the completion of recordings, animals were transcardially perfused with 100 mL of ice-cold heparinized saline followed by

300 mL of 4% paraformaldehyde in 0.1 M PBS (pH 7.4). The brains were removed and postfixed overnight at 4°C and stored in 30% sucrose in 0.1 M PBS for 72 h. Coronal sections (30 μm) were cut using a freezing microtome (Leica CM 2000R; Leica Microsystems Inc., Chantilly, VA, USA) and stored in cryoprotectant solution (15% glucose, 30% ethylene glycol and 0.04% sodium azide in 0.05 M PBS, pH 7.4) at −20°C until further processing. Serial sections from frontoparietal cortex and the striatum (between 0.5 and 1.00 mm anterior to bregma) were either Nissl-stained or processed for the histochemical visualization of AChE-positive fibers in the cortex or CHT-immunoreactivity (IR). Sections depicting the BF (1.30–1.50 mm posterior to bregma) were processed only for CHT-IR. Nissl-stained sections were produced for verification of microelectrode placements. Loss of cholinergic projections to the cortex was verified and semiquantified (below) on the basis of sections revealing the density of AChE-positive fibers in the cortex. Brain sections for AChE staining were processed using Tago's method (Tago *et al.* 1986). AChE-positive fiber density in the frontoparietal cortex was quantified using a grid counting technique as described earlier (McGaughy *et al.* 1996; Burk *et al.* 2002) using a Leica DM 4000B digital microscope (Nuhsbaum, McHenry, IL, USA). AChE-positive fibers were counted in layers III/IV (0.16 mm^2) at 400× magnification (see Fig. 1c for an illustration of the sampling area) and expressed as an average count from three sections. Note that this method was not intended to generate absolute and bias-free counts but an estimate of the 192-SAP-induced decrease in the density of the cholinergic innervation of the frontoparietal recording region.

CHT-IR

Free-floating sections stored in cryoprotectant solution were thawed and processed for CHT-IR. Sections were rinsed twice in 0.1 M Tris-buffered saline (TBS) for 5 min, incubated with blocking buffer (10% goat serum in 0.1 M TBS) with constant shaking for 60 min followed by overnight incubation with rabbit anti-CHT antibody diluted 1 : 350 in dilution buffer (0.1 M TBS containing 1% goat serum and 0.1% triton X-100) at 4°C. The following day, sections were washed in wash buffer (0.1 M TBS containing 0.1% triton X-100) four times for 5 min and incubated with 1 : 250 diluted Alexa Fluor® 488 conjugated goat anti-rabbit IgG (Molecular Probes) for 2 h at 25°C. After four 5-min rinses with wash buffer, the sections were mounted on gelatin-coated slides and coverslipped with Prolong-Gold antifade reagent. Omission of either primary or secondary antibody from this procedure eliminated CHT-IR. Sections were analyzed using a Leica DM4000B fluorescent microscope equipped with a SPOT Digital Camera and using SPOT software (Diagnostics Inc., Sterling Heights, MI, USA) and processed for quantitative image analysis using NIH IMAGE analysis software 'IMAGEJ' (http://rsb.info.nih.gov/ij). The density of CHT-IR in frontoparietal cortex was expressed as the percentage of IR-positive pixels in the analyzed area (counting area, 0.16 mm^2; see Fig. 1d). Digitized images were processed in binary mode and threshold levels were adjusted to enhance the visibility of either CHT-immunoreactive fibers or cell bodies uniformly among all sections with the help of a macro created in the software (see Fig. 1d). Furthermore, the number of CHT-immunopositive neurons was counted in the BF (1.0 mm^2) and, for control purposes, striatum (1.96 mm^2; see Fig. 1d). In all cases, average counts were based on counts from three sections per region and per animal. Again, quantification of CHT-IR was not intended to generate absolute numbers but estimates of the lesion-induced decrease in the density of CHTs in the cortex and CHT-immunopositive cells in the BF.

Synaptosomal uptake assays

Synaptosomal assays were conducted in order to determine HC-3-sensitive choline uptake under conditions that approach the total extracellular choline concentration following choline pressure ejections *in vivo,* taking into account basal extracellular choline concentration determined also *in vivo.* Choline transport assays were carried out in synaptosomes prepared from rat frontoparietal cortex with minor modifications from the method described earlier (Gates *et al.* 2004). Briefly, animals ($n = 6$) were decapitated under urethane anesthesia (1.5 g/kg; i.p). The brains were quickly removed and the frontoparietal cortex was dissected out from both hemispheres on ice-cold surface. The tissues from the two hemispheres were pooled and homogenized in 0.32 M sucrose. The homogenate was centrifuged at 1000 *g* for 4 min at 4°C. A crude synaptosomal fraction was obtained by spinning the resulting supernatant at 12 500 *g* for 15 min. The synaptosomal pellet was re-suspended in Kreb's bicarbonate buffer (KBB) containing 118 mM NaCl, 4.7 mM KCl, 1.2 mM KH_2PO_4, 25 mM $NaHCO_3$, 1.7 mM $CaCl_2$, 10 mM glucose supplemented with 100 μM AA, 10 μM physostigmine and bubbled with 95 : 5 mixture of O_2 : CO_2. Protein content was determined by Lowry's method using a commercially available kit (Sigma). The synaptosomal suspension was divided into two fractions and choline uptake assays were carried out in the absence and presence of a choline concentration (5 μM), which reflected the results of the *in vivo* determination of basal choline concentration (see Results). Aliquots (50 μL) of the synaptosomal suspension from fraction 1 were mixed with either 50 μL of KBB or KBB containing 10 μM of HC-3. Choline transport was initiated by incubating 6 μM of [^{3}H]choline at 37°C for 5 min in a shaking water bath. The uptake was terminated by transferring the tubes to ice bath followed by rapid filtration using a tissue harvester (Brandel Inc., Gaithersburg, MD, USA). In order to assess choline uptake under conditions that mirrored the extracellular concentrations of choline determined *in vivo,* and following the addition of exogenous choline in the *in vivo* experiments, aliquots from fraction 2 were pre-incubated with KBB containing 5 μM choline at 37°C for 3 min. Subsequent methods were identical to the procedures described for fraction 1 above. At all steps, the final choline concentration in the synaptosomal suspensions was maintained at 5 μM. All uptake assays were carried out in triplicate with [^{3}H]choline containing ∼10% labeled choline. Radioactivity counts were converted into [^{3}H]choline concentration derived from standard plots and values were normalized to synaptosomal protein concentration.

Statistical analyses

Statistical analyses were performed using SPSS/PC+ V. 13.0 (SPSS, Chicago, IL, USA). Repeated measure ANOVAS, with Huynh–Feldt correction for degrees of freedom where necessary, were employed to analyze the effects of HC-3 (signal amplitudes/injection volume; T_{20-60}; T_{40-80}; T_{C1}; T_{C2}). *Post-hoc* multiple comparisons were conducted using the least significant difference (LSD) test (alpha = 0.05 for all statistical analyses). As only the higher concentration of

HC-3 was tested in lesioned animals, group-based comparisons of clearance data, as well as histological and immunohistochemical data, were carried out using planned, two-tailed, unpaired Student's *t*-tests. Correlations between clearance data and CHT-IR were carried out by determining Pearson's *r* and testing correlation coefficients for statistical significance. Exact *p*-values are reported as per recommendations by Greenwald and colleagues (Greenwald *et al*. 1996).

Results

Microelectrode calibration and basal cortical extracellular choline concentration

Microelectrodes properties (calibration data)

The microelectrodes ($n = 20$) used for these experiments displayed a background current of 66.44 ± 4.87 pA and a sensitivity of 6.58 ± 0.07 pA/μM of choline. Table 1 depicts LOD, R^2, selectivity of choline to AA (Choline : AA) and DA (Choline : DA) in single and self-referencing modes. These calibration parameters indicated that the microelectrodes were capable of detecting choline in a sensitive and selective manner, and that the responses of the electrodes to increasing concentrations of choline (up to 80 μM) were highly linear (see Table 1).

Basal extracellular choline concentration in the cortex measured in vivo

Choline-sensitive microelectrodes were employed to determine, *in vivo,* the concentration of extracellular choline in the cortex (see Materials and methods for details). In intact animals, the concentration of extracellular choline in the frontoparietal cortex was 4.85 ± 1.12 μM ($n = 6$). This value is similar to basal brain extracellular choline concentration determined by using microdialysis (Koppen *et al*. 1996; Klein *et al*. 2002).

Clearance of exogenous and endogenous choline via HC-3-sensitive mechanisms in the cortex *in vivo*

HC-3-induced decreases in the clearance of exogenous choline

Exogenous choline (5 mM) is rapidly cleared via HC-3-sensitive mechanisms. Figure 2(a) shows representative traces depicting self-referenced signals in response to pressure ejections of choline in the presence and absence of HC-3 (see Table 2 for data). As described in Materials and methods, the volume of pressure ejections of choline when co-injected with HC-3, were adjusted to yield amplitudes similar to those generated by choline alone (20–25 μM), in order to avoid amplitude-based confounds in the calculation

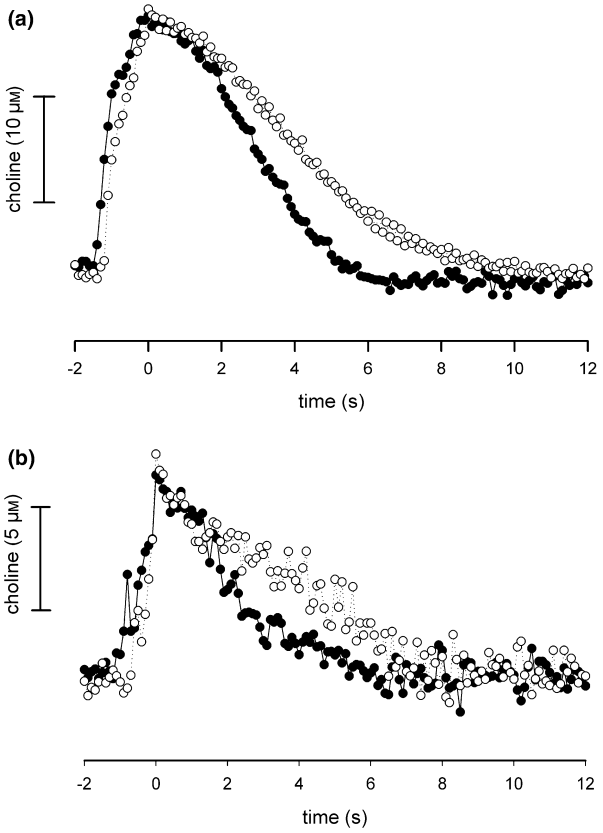

Fig. 2 Representative, self-referenced traces depicting choline signals produced by pressure ejection of choline (5 mM) or KCl (70 mM), and attenuation of clearance of exogenous as well as endogenous choline by hemicholinium-3 (HC-3, 10 μM; see Table 2 for the effects of both concentrations of HC-3 and for clearance data). The more variable electrode response in (b), relative to (a), presumably reflects the detection of choline from endogenous sources. KCl-induced choline signals were previously demonstrated to be attenuated by the co-administration of either an acetylcholinesterase inhibitor or tetrodotoxin, indicating that potassium-induced signals reflect choline hydrolyzed from newly released acetylcholine (Parikh *et al.* 2004). Legend for panel (a): ●, choline 5 mM; ○, choline 5 mm + HC-3 10 μM. Legend for panel (b): ●, KCl 5 mM; ○, KCl 5 mm + HC-3 10 μM.

Table 1 Electrode properties (calibration data)

Analysis mode	LOD (nM)	R^2	Choline : AA	Choline : DA
Single	189.56 ± 25.1	0.991 ± 0.004	327.13 ± 60.13	0.162 ± 0.044
Self-referencing	205.09 ± 0.4	0.992 ± 0.003	266.96 ± 42.81	> 1000 ± 0.0

Data are based on 20 microelectrodes used for these experiments (mean ± SEM); LOD, limit of detection; R^2, linearity of the response of the microelectrode to increasing concentrations of choline; AA, ascorbic acid; DA, dopamine.

Table 2 Effect of HC-3 on the clearance of exogenous choline (5 mM)

Drugs	Signal amplitude/ ejected volume (nM/nL)	T_{20-60} (ms)	T_{c1} (μM/s)	T_{40-80} (ms)	T_{c2} (μM/s)
Choline (5 mM) + vehicle	94.65 ± 5.63	2117 ± 180	4.84 ± 0.50	2196 ± 170	4.39 ± 0.50
Choline (5 mM) + HC-3 (1 μM)	111.60 ± 6.41***	2337 ± 171*	4.28 ± 0.42	3021 ± 245**	3.46 ± 0.37**
Choline (5 mM) + HC-3 (10 μM)	134.92 ± 9.78***,b	2838 ± 128**,a	3.38 ± 0.31**,a	4054 ± 419**,a	2.59 ± 0.31***,a

All data are expressed as mean ± SEM ($n = 8$). Statistical analyses were carried out using repeated measures ANOVA followed by *post-hoc* pairwise comparisons analysis using the LSD test; *$p < 0.05$, **$p < 0.01$, ***$p < 0.001$ vs. choline (5 mM); [a]$p < 0.05$, choline (5 mM) + HC-3 (1 μM) vs. choline (5 mM) + HC-3 (10 μM); [b]$p < 0.01$, choline (5 mM) + HC-3 (1 μM) vs. choline (5 mM) + HC-3 (10 μM); see text for the justification of the calculation of the ratio between signal amplitude and ejected volume.

of uptake rate. As a blocker of a major transporter would also be expected to increase signal amplitude (Cass *et al*. 1993), signal amplitude/ejected choline volume ratios increased following co-pressure ejections of HC-3 ($F_{2,21} = 26.60$; $p = 0.001$; Table 2).

HC-3 significantly reduced the uptake rate of choline and increased the time required to clear choline; these effects were significant with respect to both phases of clearance (T_{C1}, $F_{2,21} = 7.75$, $p = 0.02$; T_{C2}, $F_{2,21} = 19.30$, $p = 0.002$; see Table 2 for results from multiple comparisons). However, significant decreases in the choline uptake rate following the smaller dose of HC-3 (1 μM) were restricted to T_{C2}, indicating that the blockade of CHTs more potently affects the later phase of clearance. Likewise, the HC-3-sensitive proportion of T_{C2} was 21% (1 μM HC-3) and 41% (10 μM), compared with 11% and 30%, respectively, for T_{C1}. Furthermore, the higher dose of HC-3 increased the time required to clear 40–80% of the peak choline concentration by 1858 ms, compared with 721 ms for T_{20-60} (see Table 2).

HC-3-induced decreases in the clearance of endogenous choline

Previous studies demonstrated that choline signals produced by KCl are attenuated by co-administration of either an esterase inhibitor or tetrodotoxin, indicating that KCl-induced choline signals reflect choline derived from hydrolysis of newly released ACh (Parikh *et al*. 2004). Figure 2(b) illustrates a KCl-induced choline signal and the decrease in clearance of such a signal by HC-3 (see Table 3 for a summary of findings).

Administration of 70 mM KCl elicited choline signal amplitudes averaging 12.65 ± 0.76 μM. Inspection of the representative traces shown in Fig. 2(b) appears to indicate a greater variability of the electrode response to KCl when compared with the detection of exogenous choline, presumably reflecting the two physiological processes responsible for the depolarization-induced choline signal generation (ACh release and hydrolysis; Parikh *et al*. 2004).

In contrast to experiments on the clearance of exogenous choline (above), it was not necessary to decrease the volume of KCl when co-injected with HC-3 in order to maintain similar amplitudes. Thus, amplitude/ejection volume ratios did not change following co-injection of HC-3 ($F_{2,12} = 0.81$, $p = 0.52$, see Table 3; see Discussion for implications).

HC-3 significantly reduced the uptake of endogenously derived choline for both the earlier and the later phase of clearance (T_{C1}, $F_{2,11} = 8.661$, $p = 0.05$; T_{C2}, $F_{2,12} = 18.356$, $p = 0.021$). Multiple comparisons (see Table 3) indicated that T_{C1} was only affected by the higher concentration of HC-3 (30% decrease). Both concentrations of HC-3 decreased the uptake rate for the later phase of clearance (43% decrease after 10 μM HC-3).

The time required to clear 20–60% of depolarization-generated endogenous choline was not significantly affected by HC-3 ($F_{2,12} = 2.08$, $p = 0.27$). In contrast T_{40-80} was significantly increased by HC-3 ($F_{2,12} = 12.32$, $p = 0.036$), by 1367 ms (mean difference).

Table 3 Effect of HC-3 on clearance of potassium-evoked choline signals

Drugs	Signal amplitude/ ejected volume (nM/nL)	T_{20-60} (ms)	T_{c1} (μM/s)	T_{40-80} (ms)	T_{c2} (μM/s)
KCl (70 mM) + vehicle	62.14 ± 4.61	2020 ± 95	2.63 ± 0.34	2653 ± 203	2.49 ± 0.27
KCl (70 mM) + HC-3 (1 μM)	58.32 ± 5.19	2393 ± 165	2.31 ± 0.41	3280 ± 279**	2.01 ± 0.28*
KCl (70 mM) + HC-3 (10 μM)	61.39 ± 5.16	2653 ± 395	1.84 ± 0.24*	4020 ± 498**,a	1.43 ± 0.13**,a

All data are expressed as mean ± SEM ($n = 5$). Statistical analysis was carried out using repeated measures ANOVA followed by *post-hoc* pairwise comparisons analysis using the LSD test; *$p < 0.05$, **$p < 0.01$ vs. KCl (70 mM); [a]$p < 0.05$, KCl (70 mM) + HC-3 (1 μM) vs. KCl (70 mM) + HC-3 (10 μM); see text for the justification of the calculation of the ratio between signal amplitude and ejected volume.

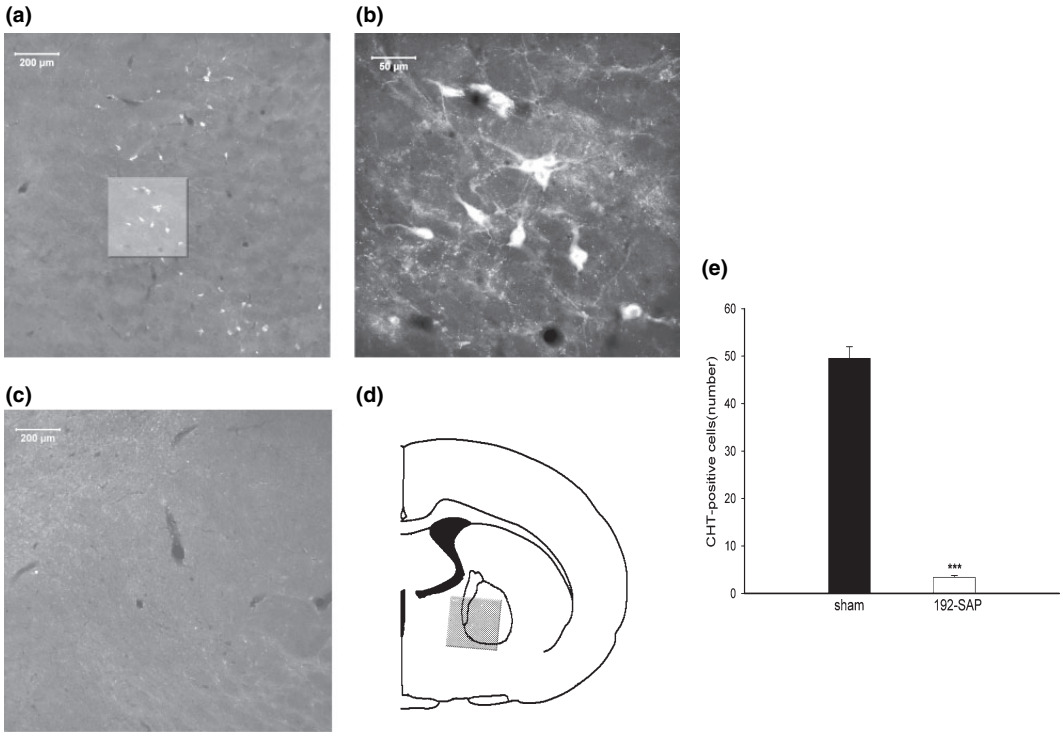

Fig. 3 The verification of the loss of cholinergic neurons as a result of the infusion of 192-IgG saporin (192-SAP) at the level of the BF and as indicated by the presence/absence of CHT-immunoreactive neurons. (a) Low-magnification microphotograph (200 μm scalebar inserted) showing CHT-positive neurons organized along the medial wall of the globus pallidus (nucleus basalis of Meynert; nbM). The location of this region is indicated on a schematic coronal section in (d). The highlighted region in (a) is magnified in (b) (50 μm scalebar inserted) and exemplified the magnocellular cholinergic neurons that are characteristic for the nbM and predominantly project to the cortex. Panel (c) illustrates the almost complete absence of CHT-IR in the nbM region following infusions of 192-SAP. (e) Estimates of CHT-positive neurons (see Materials and methods) indicated extensive loss of these neurons as a result of 192-SAP lesions (white bar) as compared with sham (black bar) (***$p < 0.001$).

Effects of cholinergic deafferentation on choline clearance

The loss of cholinergic projections to the recording field, produced by infusions of the immunotoxin 192-SAP into the BF, was expected to result in a decrease in choline clearance as a result of the loss of cholinergic terminals, and thus a decrease in the number of CHTs available for choline uptake. The immunotoxin has been widely demonstrated to produce a selective loss of cholinergic neurons (e.g. Wiley *et al*. 1991; Holley *et al*. 1994; Pizzo *et al*. 1999); as CHTs are selectively expressed by cholinergic neurons (e.g. Misawa *et al*. 2001), the effects of the lesions on choline clearance can be largely attributed to the decrease in CHT availability.

Histological analyses

Figure 3 illustrates the effects of lesions on CHT-positive cells in the BF. Lesion-induced decreases in AChE-positive fiber density and CHT-IR in the cortical recording region are illustrated in Figs 4 and 5, respectively.

The lesion resulted in a marked loss of CHT-IR cell bodies in the BF (Fig. 3). Semi-quantitative cell counts indicated a significant reduction of CHT-IR cells in the nBM/SI region [$t_{(1,13)} = 17.97$; $p < 0.001$]. In the frontoparietal recording region, AChE-positive fiber density was markedly decreased in lesioned animals [Fig. 4; $t_{(1,13)} = 14.18$; $p < 0.001$]. The analyses of the effects of the lesions on choline clearance described below were based on data from a total of seven animals with decreases in frontoparietal AChE-positive fiber density that were >80% when compared with the mean count from sham-lesioned controls ($n = 8$). Frontoparietal CHT-IR was also decreased by the lesion [controls, 1.41 ± 0.16 (percentage immunoreactive pixels); lesioned, 0.29 ± 0.07; $t_{(1,13)} = 6.521$; $p < 0.001$; Fig. 5].

Basal extracellular choline concentrations

Brain levels of choline are protected by potent homeostatic mechanisms (Klein *et al*. 1998; Klein *et al*. 2002) and thus, loss of cholinergic terminals was not expected to affect basal extracellular concentrations (see also Zapata *et al*. 2000). The results confirmed that basal extracellular choline concentrations in the frontoparietal cortex of lesioned animals did not differ from controls [controls,

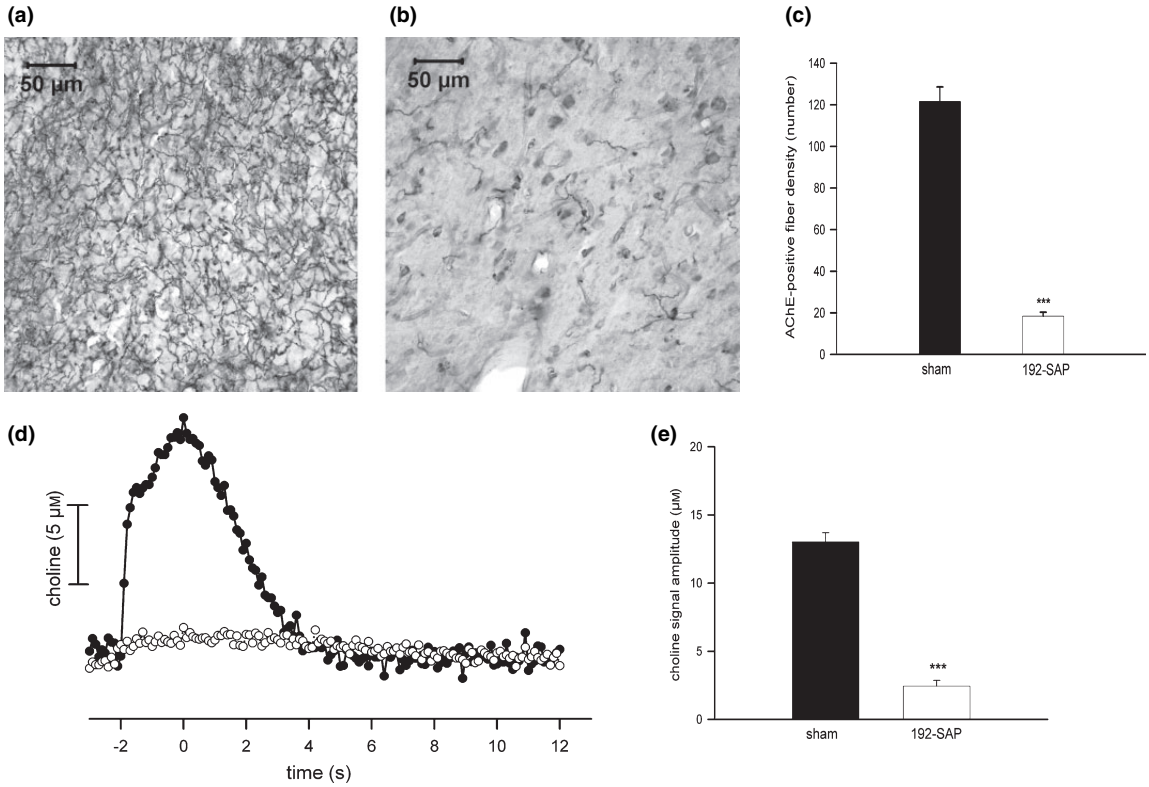

Fig. 4 Effects of loss of cholinergic input to the recording region on KCl-induced choline signals. Panels (a) and (b): AChE-positive fiber densities in the recording region from an intact (a) and a lesioned animal (b) (50 μm scalebars are inserted). Comparison between cholinergic fiber densities indicated a highly significant, >80% reduction in the density of cholinergic inputs to the recording region as a result of injections of 192-IgG saporin (192-SAP, ***p < 0.001). (d) Example of a KCl-induced signal in a sham (●) and a 192-SAP-lesioned (○) animal. As a result of the extensive decrease of cholinergic terminals, KCl-induced signal amplitudes were significantly decreased in 192-SAP lesioned (white bars) as compared with sham (black bars) animals (e). These data confirm that the demonstration of potassium-induced choline signals *in vivo* depends on the presence and integrity of cholinergic terminals.

4.85 ± 1.12 μM; lesioned, 6.83 ± 0.96 μM; $t_{(1,10)} = 1.34$; $p = 0.21$].

Cholinergic deafferentation-induced attenuation of KCl-induced choline signals

Determination of KCl-induced choline signal amplitudes served to verify the degree of cholinergic terminal loss in the recording area. Figure 4(d) shows representative self-referenced traces of cortical choline signals generated by pressure ejections of 200 nL KCl (70 mM) in a sham-lesioned and a deafferented animal. Potassium-evoked choline signals were significantly attenuated by the loss of cholinergic projections [$t_{(1,13)} = 13.32$; $p < 0.001$]; on average, amplitudes were decreased by 81% relative to controls (see Fig. 4e).

Clearance of exogenous choline following loss of cholinergic terminals

Because of the expectedly low residual amplitudes of KCl-induced choline signals in the frontoparietal cortex of lesioned animals (above), the effects of the lesion on choline clearance were only assessed with respect to clearance of exogenous choline (Fig. 5). Similarly to the experiment on the effects of choline plus HC-3 (above), following the lesion, choline volumes needed to be reduced in order to produce comparable amplitudes, resulting in an increase in the amplitude/ejected volume ratio (sham, 94.65 ± 5.63 nM/nL; lesion, 127.97 ± 5.98 nM/nL; $t_{(1,13)} = 3.94$; $p = 0.01$). Therefore, pressure ejections of choline (5 mM) produced identical choline signal amplitudes in sham-lesioned and deafferented rats [21.96 ± 0.52 μM and 23.07 ± 0.79 μM; $t_{(1,13)} = 1.25$; p = 0.27; Fig. 5d].

Loss of cholinergic inputs resulted in a significant decrease in choline clearance that manifested with respect to the later phase of clearance [T_{C2}, $t_{(1,13)} = 11.52$, $p = 0.009$, Fig. 5e; T_{40-80}, $t_{(1,13)} = 12.431$, $p < 0.001$, Fig. 5f]. The effects of the lesion on T_{C1} and T_{20-60} remained insignificant (both $p > 0.05$; Figs 5e and f). Descriptively, the loss of cholinergic inputs reduced the choline uptake rate (T_{C2}) by 37% and increased the T_{40-80} by 1686 ms. Because the lesion produced a marked reduction in the number of CHTs, co-administration of HC-3 (10 μM) failed to produce additional decreases in choline clearance in lesioned animals (all

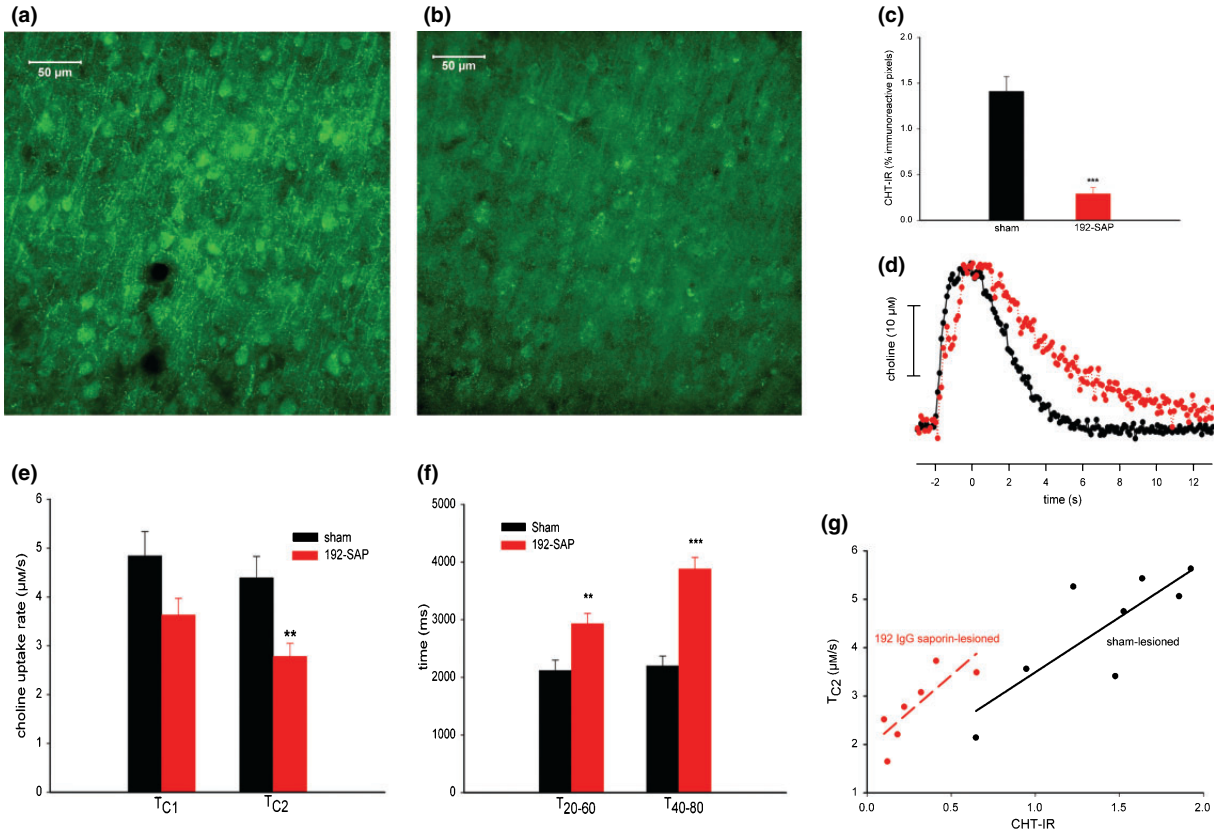

Fig. 5 Effects of loss of cholinergic inputs to the recording area on choline clearance. a, b photomicrographs of the frontoparietal sampling region (see fig. 1d for location of the sampling area) showing CHT-IR on a section of a sham-operated animal (a) and a 192-SAP-lesioned animal (b; 50 µm scales are inserted). The lesion resulted in a significant reduction of CHT-IR (see bar graph in c). (d) depicts two representative raw (non-self-referenced) traces showing exogenous choline clearance in the frontoparietal cortex of a sham (black circles) and a lesioned animal (gray circles). Choline uptake rate was decreased in lesioned (gray bars) as compared to sham (black bars) animals; the effect reached significance in the later phase of clearance (T_{C2} see e). The 192-SAP lesion (gray bars) resulted in significant increase in the time required to clear choline for both phases of clearance as compared to sham (black bars) animals (**, $p < 0.01$; ***, $p < 0.001$). (g) illustrates the significant correlations found betweem CHT-IR and T_{C2} in the frontoparietal cortex of sham-operated ($r = 0.81$) and 192-SAP lesioned animals ($r = 0.40$).

$p > 0.05$; data not shown). The failure of HC-3 to produce additional retardation of choline clearance in lesioned animals further supports the selectivity of the effects of this CHT blocker.

Correlations between histological, immunohistological measures and choline clearance

Frontoparietal CHT-IR and T_{C2} choline uptake rate were significantly correlated (Fig. 5g; sham-lesioned, $r = 0.81$, $p = 0.01$; lesioned, $r = 0.40$, $p = 0.03$). The finding that CHT-IR and T_{C2} were significantly correlated in control animals indicates a substantial variability in the density of frontoparietal CHTs between individual intact animals, and that such variability is of functional significance. Furthermore, in lesioned animals, residual frontoparietal CHT-IR and AChE-positive fiber densities were significantly correlated ($r = 0.92$, $p = 0.003$; data not shown), substantiating the assumption that the decrease in CHT-IR was directly associated with the decrease in cholinergic innervation of the recording area.

KCl-induced choline signals in the striatum of lesioned animals

The selectivity of the lesion effects were also confirmed by the finding that CHT-IR cell counts in the striatum did not differ significantly between the two groups [$t_{(1,13)} = 0.44$, $p = 0.66$; Fig. 6]. In order to substantiate the regional selectivity of the lesion, choline-sensitive microelectrodes were lowered into the striatum and choline amplitudes were recorded following pressure ejections of 80 nL of KCl (70 mM). The amplitudes were found to be identical in lesioned and control animals (controls, 12.06 ± 1.58 µM; lesioned, 10.58 ± 1.67 µM; $t_{(1,4)} = 0.65$; $p = 0.55$; Fig. 6d].

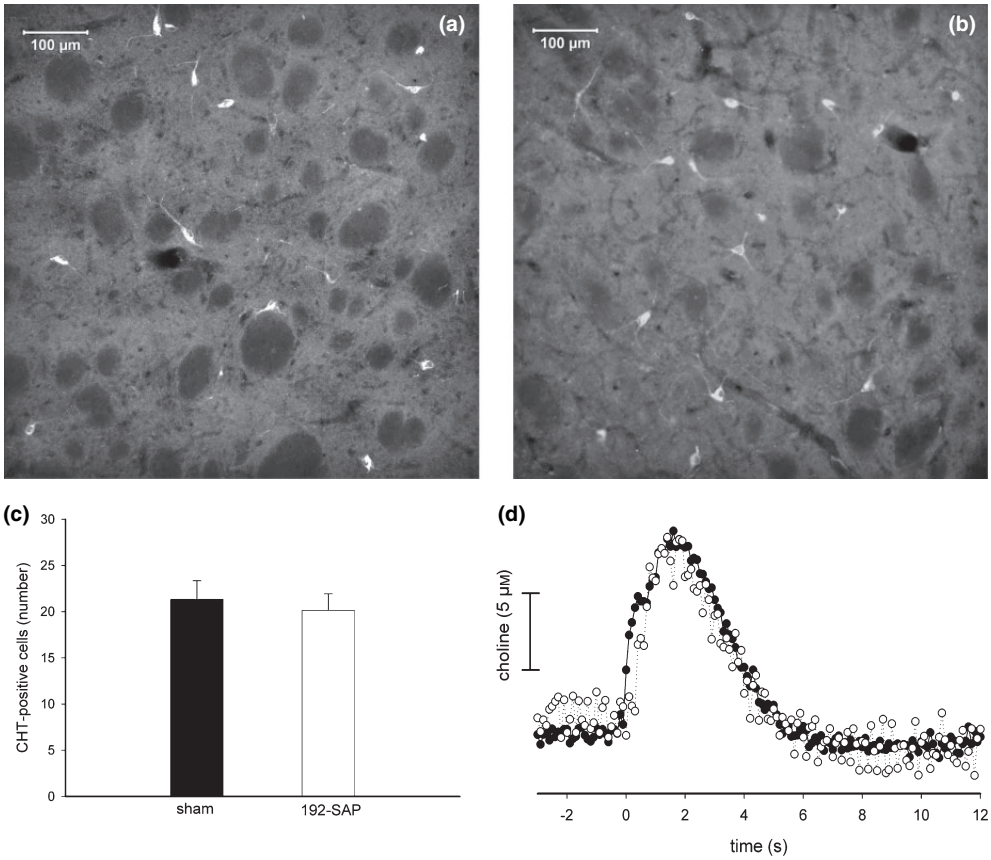

Fig. 6 Striatal CHT-IR and KCl-induced choline signals were determined in order to substantiate the selectivity of the effects of infusions of 192-SAP on the BF cholinergic projection system. Panels (a) and (b) illustrate striatal cholinergic interneurons visualized by CHT-IR. Estimates of the density of these neurons did not indicate a difference between sham (black bar) and lesioned (white bar) rats (c). Likewise, identical choline signals in response to a depolarizing stimulus (KCl) were observed in the striatum of lesioned (○) and control (●) animals, as exemplified in (d).

Synaptosomal choline uptake under basal choline concentrations reflecting *in vivo* conditions

For the *in vivo* experiments described above, exogenous choline (5 mM) was pressure-ejected into the extracellular space, which already contained 4.85 µM choline (basal choline concentration; above). This experiment was designed to substantiate the HC-3-sensitive component of [^{3}H]choline uptake *in vitro* by synaptosomes, under conditions that approached the choline extracellular concentrations following choline pressure ejections *in vivo*. Furthermore, the effects of local pressure-ejections are associated with diffusion of the substrate away from the electrode; such diffusion is inherent to the method but is of no significance in *in vitro* synaptosomal assays. Thus, evidence from this experiment assists in interpreting the quantitative results generated by the *in vivo* studies described above. A crude synaptosomal fraction was obtained from frontoparietal cortex and pre-incubated in either the absence or presence of 5 µM choline. [^{3}H]Choline uptake was determined in either the presence or absence of 10 µM HC-3. As increases in choline concentrations results in the dilution of the concentration of [^{3}H]choline, saturation kinetics for choline uptake (K_m, V_{max}) were not determined; rather, choline uptake was measured at one concentration of HC-3. In the absence of 5 µM choline in the pre-incubation medium, HC-3 suppressed choline uptake by 74.90 ± 1.48%. Following pre-incubation of synaptosomes with 5 µM choline, HC-3-induced inhibition of choline uptake was 43.62 ± 3.51% [without HC-3, 30.31 ± 3.97 pmol/5min/mg protein; with HC-3, 17.08 ± 1.62 pmol/5 min/mg protein; $t_{(1,10)} = 8.02$; $p < 0.001$]. The proportion of choline uptake that was sensitive to HC-3, measured in the presence of choline concentrations reflecting the concentration observed *in vivo,* corresponded with the HC-3-sensitive component of T_{C2} observed *in vivo*. Thus, this finding substantiates the proportion of the HC-3-sensitive component of choline clearance observed *in vivo.* This result also indicates that the diffusion of the substrate away from the electrode does not substantially undermine the *in vivo* findings.

Discussion

These experiments utilized *in vivo* and *in vitro* methods in order to determine changes in extracellular choline concentration and high-affinity CHT function in the cortex *in vivo*. We report six main findings and will discuss their implications below.

(i) *In vivo*, cortical choline uptake via HC-3-sensitive mechanisms represents a main mechanism for the rapid clearance of local increases in extracellular concentrations of choline.

(ii) CHTs contribute mostly to the clearance of choline during the latter of the two components of the clearance phase (T_{C2}). The CHT-mediated clearance during this latter component did not fundamentally depend on the source of choline (depolarization-induced increases of endogenous choline concentrations versus exogenous choline).

(iii) Following 192-SAP-induced cholinergic deafferentation of the recording region, depolarization-induced choline signal amplitudes were almost completely attenuated, confirming that the demonstration of KCl-induced choline signals requires acetylcholine (ACh) release and hydrolysis.

(iv) In animals with a loss of cholinergic projections to the recording region, the decrease in clearance of exogenous choline corresponded with the effects of HC-3 in intact animals. Furthermore, the density of CHTs in the recording region of lesioned animals correlated significantly with the choline uptake rate in the later clearance phase. In intact animals, CHT-immunoreactivty in the recording region also was highly correlated with choline uptake rate (T_{C2}); these data indicate that there is considerable interindividual variability in the density of CHTs in intact animals and that this variability is of functional significance.

(v) Basal extracellular concentration of choline *in vivo* was determined to be 4.85 μM. Loss of cortical cholinergic inputs to the recording region did not affect basal choline concentration.

(vi) CHT-mediated choline uptake was also determined *in vitro* using a synaptosomal uptake assay and conditions that mirror extracellular choline concentrations following choline pressure-ejections *in vivo*. As diffusion of the substrate away from the electrode surface *in vivo* does not represent a variable in synaptosomal assays, collectively these findings support the conclusion that approximately 40% of choline clearance is a result of choline uptake by CHTs.

The attribution of the effects of HC-3 to the inhibition of uptake via CHTs requires comment. HC-3 is a highly selective, highly potent, competitive inhibitor of CHTs (K_i = 1–100 nM; Lockman and Allen 2002). In contrast, the concentrations of HC-3 required to affect low-affinity choline transport ($K_i \sim 100$ μM) were not reached in the present *in vivo* experiments. Based on the ratio between the concentration of pressure-ejected choline and the concentration of choline detected by the electrode, and ignoring the different physico-chemical properties of HC-3, we can cautiously estimate that the highest concentration of pressure-ejected HC-3 (10 μM) may have yielded <100 nM concentrations in the recording field. A more convincing argument in support of the selectivity of the effects of HC-3 is derived from data obtained from animals with a loss of cholinergic projections to the recording field. Loss of cholinergic terminals, which selectively express CHTs (e.g. Misawa *et al*. 2001; Ferguson *et al*. 2003; Kus *et al*. 2003), resulted in a decrease in choline clearance that corresponded well with the effects of HC-3 in intact rats, indicating that the effects of HC-3 specifically reflected the inhibition of CHTs (see also Freeman *et al*. 1979; Chatterjee *et al*. 1987; Saltarelli *et al*. 1987; Ferguson *et al*. 2003). Furthermore, in lesioned animals, HC-3 was no longer able to generate further inhibition of clearance. This finding further excludes the possibility that the effects of HC-3 were caused by mechanisms unrelated to the inhibition of CHTs located on cholinergic terminals.

A second methodological issue that deserves comment concerns the effects of either HC-3 pressure ejections or loss of cholinergic terminals on choline signal amplitude. Reduced clearance would be expected to be associated with increases in signal amplitude, similar to the evidence described in Cass *et al*. (1993). As described in the Materials and methods section, volumes of pressure ejections were adjusted to yield identical amplitudes in order to ensure that the proportion of choline cleared by the substrate-regulated low-affinity choline transporter remained roughly similar across HC-3 concentrations, and to minimize amplitude-based biases in the calculation of clearance rates. As would be expected, the volume of pressure-ejected exogenous choline needed to be decreased when co-injected with HC-3, to achieve amplitudes similar to those produced by choline alone (see the increase in amplitude/volume ratios in Table 2).

Unexpectedly, such volume adjustment was not required in experiments assessing the clearance of endogenous choline following KCl pressure ejections (Table 3). As the efficacy of HC-3 to attenuate choline clearance did not differ between KCl-induced increases in choline concentrations and increases caused by choline pressure ejections, the basis for a lack of effects of HC-3 on KCl-induced signal amplitudes remains unclear.

Diffusion of substrate away from the recording electrode represents a variable that is difficult to control in *in vivo* experiments using substrate-sensitive microelectrodes. Although quantitative diffusion models (e.g. Nicholson 1985) assisted greatly in substantiating the conclusion that dopamine transporters are largely responsible for dopamine clearance (Cass *et al*. 1993), application of such models to the present data is limited by the unknown proportion of

choline clearance associated with the low-affinity choline transporter. We are not aware of an experimental approach available for determining the contribution of the low-affinity transporter to choline clearance. Therefore, the results from our *in vitro* synaptosomal assays are relevant to the interpretation of the *in vivo* data. Because diffusion (of the substrate away from the electrode) does not represent a variable in measurements of choline uptake using synaptosomal assays, and although the proportion of low-affinity choline uptake transporters in a crude synaptosomal fraction is unlikely to reflect the density of low-affinity choline transporters *in vivo*, the observation that the HC-3-sensitive component of choline uptake *in vitro* agrees quantitatively with the HC-3-sensitive component of choline clearance measured *in vivo* (40–43% of overall clearance) appears informative. Moreover, this estimate appears to be in general agreement with earlier conclusions concerning the proportion of choline recycled for ACh synthesis (Collier and Katz 1974).

The finding that relatively high exogenous choline concentrations were cleared as rapidly and as extensively as KCl-induced increases in extracellular choline, via CHTs, suggests that the capacity of CHTs does not exclusively depend on cholinergic neuronal activity. For this discussion, it is important to first exclude the possibility that increases in choline concentrations depolarized cholinergic terminals. Choline has also been suggested to act as an agonist at α_7 nicotinic receptors (Alkondon *et al*. 1997). As nicotinic receptor stimulation elicits choline signals (Parikh *et al.* unpublished observations), choline-induced depolarization of cholinergic neurons, either directly or involving for example the release of excitatory amino acids (Rousseau *et al*. 2005), could have contributed to the rapid CHT-mediated clearance of exogenous choline. However, given the low micromolar concentrations of basal extracellular choline concentrations, and the micromolar choline signal peak amplitudes observed following both KCl and choline pressure ejections, it seems highly unlikely that the millimolar concentrations of choline required to stimulate nicotinic receptors (Alkondon *et al*. 1997) were reached in these experiments. Indeed, as it is difficult to envision local extracellular, endogenous choline concentrations higher than those seen following KCl-induced depolarization, reflecting increases in extracellular ACh by several hundreds of percent (Herzog *et al*. 2003), it is not clear whether concentrations required to stimulate nicotinic receptors can occur *in vivo* (Ulus *et al*. 1988). This view is also supported by the observation that choline signals evoked by even higher concentrations of choline (20 mM) were not affected by high concentrations of neostigmine (100 mM), indicating that choline from endogenous sources does not contribute to the signal recorded following such choline pressure ejections (Parikh *et al*. 2004).

The present data indicate that the rate of clearance of exogenous choline (peak amplitudes, 20–25 μM) via CHTs does not differ fundamentally from the clearance of endogenous choline, generated as a result of terminal depolarization. The suggestion that a low-affinity state of the CHT (K_D = 22.8 nM; Chatterjee *et al*. 1987) represents the functionally active form of the high-affinity precursor uptake system (Chatterjee *et al*. 1987) corresponds with the ability of the CHT to clear high extracellular concentrations of exogenous choline, specifically if it is also speculated that increased extracellular choline concentrations trigger a conformational change to the low-affinity state. However, our findings on exogenous choline clearance do not suggest that a tight coupling between high-affinity precursor uptake and ACh synthesis (e.g. Atweh *et al*. 1975) represents an exclusive mode of CHT capacity regulation. Furthermore, our results on the effects of KCl suggest that endogenous choline concentrations, even under conditions of extreme activation of cholinergic neurons, may rarely exceed 10–15 μM, and thus appear to stay well within estimates of the limits of the capacity of CHTs (Ferguson and Blakely 2004). These data also indicate that the conditions which necessitate increased translocation of the CHT to plasma membranes (Ferguson and Blakely 2004; Apparsundaram *et al*. 2005) deserve more research.

Concerns about the degree to which high-affinity choline uptake is coupled to ACh synthesis and release have been raised previously (e.g. Kessler and Marchbanks 1979; Collier and Ilson 1977). Although information about the regulation of choline acetyltransferase (ChAT) and the vesicular transporter remains incomplete, it is generally believed that these steps do not significantly contribute to the rate-limiting mechanisms of ACh synthesis (Yamamura and Snyder 1972). Therefore, it may be assumed that CHT-mediated transport of choline, including the transport of choline of exogenous origin, serves as a precursor for ACh synthesis. Results from prior microdialysis experiments also indicated that increased choline concentrations, including those from dietary sources, are taken up a HC-3-sensitive mechanisms and yield increases in ACh release (Cohen and Wurtman 1976; Growdon *et al*. 1977; Ulus *et al*. 1989; Koshimura *et al*. 1990; Marshall and Wurtman 1993; Ikarashi *et al*. 1997; Koppen *et al*. 1997; Vinson and Justice 1997). The present results correspond with this evidence, collectively indicating that increases in extracellular choline from exogenous sources, and not necessarily involving cholinergic neuronal activity, will be cleared by CHTs.

The notion that the CHT is regulated in part by its substrate would suggest that the functional properties of the CHT are comparable with those of other neurotransmitter transporters, such as the dopamine, norepinephrine or serotonin transporters (Cass *et al*. 1993; Zahniser and Doolen 2001; Zahniser and Sorkin 2004). If this assumption is correct, it would be important to determine whether substrate-induced trafficking, which was demonstrated for the dopamine transporter (Chi and Reith 2003), also applies

to the CHT. However, in contrast to evidence demonstrating that the dopamine transporter fully accounts for dopamine clearance (Cass *et al*. 1993; Giros *et al*. 1996; Benoit-Marand *et al*. 2000), the contribution of the low-affinity choline transporter to choline clearance *in vivo* remains unsettled.

Finally, the significant correlation between CHT-IR and choline clearance observed in intact animals suggests that the density of CHTs in the cortex varies considerably between animals, and that this variability is of functional significance. In the context of previous results indicating that cognitive performance correlated with CHT-mediated choline uptake and the density of CHTs in plasma membrane in the cortex (Apparsundaram *et al*. 2005), the present correlational results further support the possibility that CHT-mediated choline clearance serves as a marker predicting individual cognitive performance.

Acknowledgements

We thank Dr Jochen Klein (Texas Tech School of Pharmacy) and Dr Subbu Apparsundaram (University of Kentucky) for discussions concerning extracellular choline concentrations and synaptosomal uptake data. We also thank Drs G. Gerhardt, F. Pomerleau and P. Huettl (Center for Sensor Technology, University of Kentucky) for technical support and advice. Thanks also to Elise Dagenbach for comments on the final draft. The authors' research has been supported by PHS grants KO2 MH01072 NS37026, MH063114, and MH037600.

References

Alkondon M., Pereira E. F., Cortes W. S., Maelicke A. and Albuquerque E. X. (1997) Choline is a selective agonist of alpha7 nicotinic acetylcholine receptors in the rat brain neurons. *Eur. J. Neurosci.* **9**, 2734–2742.

Apparsundaram S., Martinez V., Parikh V., Kozak R. and Sarter M. (2005) Increased capacity and density of choline transporters situated in synaptic membranes of the right medial prefrontal cortex of attentional task-performing rats. *J. Neurosci.* **25**, 3851–3856.

Atweh S., Simon J. R. and Kuhar M. J. (1975) Utilization of sodium-dependent high affinity choline uptake in vitro as a measure of the activity of cholinergic neurons in vivo. *Life Sci.* **17**, 1535–1544.

Benoit-Marand M., Jaber M. and Gonon F. (2000) Release and elimination of dopamine in vivo in mice lacking the dopamine transporter: functional consequences. *Eur. J. Neurosci.* **12**, 2985–2992.

Blusztajn J. K. and Wurtman R. J. (1983) Choline and cholinergic neurons. *Science* **221**, 614–620.

Book A. A., Wiley R. G. and Schweitzer J. B. (1992) Specificity of 192 IgG-saporin for NGF receptor-positive cholinergic basal forebrain neurons in the rat. *Brain Res.* **590**, 350–355.

Brandon E. P., Mellott T., Pizzo D. P. *et al.* (2004) Choline transporter 1 maintains cholinergic function in choline acetyltransferase haploinsufficiency. *J. Neurosci.* **24**, 5459–5466.

Burk J. A., Herzog C. D., Porter M. C. and Sarter M. (2002) Interactions between aging and cortical cholinergic deafferentation on attention. *Neurobiol. Aging* **23**, 467–477.

Burmeister J. J. and Gerhardt G. A. (2001) Self-referencing ceramic-based multisite microelectrodes for the detection and elimination of interferences from the measurement of l-glutamate and other analytes. *Anal. Chem.* **73**, 1037–1042.

Burmeister J. J., Palmer M. and Gerhardt G. A. (2003) Ceramic-based multisite electrode array for rapid choline measures in brain tissue. *Anal. Chimica Acta* **481**, 65–74.

Cass W. A., Zahniser N. R., Flach K. A. and Gerhardt G. A. (1993) Clearance of exogenous dopamine in rat dorsal striatum and nucleus accumbens: role of metabolism and effects of locally applied uptake inhibitors. *J. Neurochem.* **61**, 2269–2278.

Chatterjee T. K., Cannon J. G. and Bhatnagar R. K. (1987) Characteristics of [3H]hemicholinium-3 binding to rat striatal membranes: evidence for negative cooperative site–site interactions. *J. Neurochem.* **49**, 1191–1201.

Chi L. and Reith M. E. (2003) Substrate-induced trafficking of the dopamine transporter in heterologously expressing cells and in rat striatal synaptosomal preparations. *J. Pharmacol. Exp. Ther.* **307**, 729–736.

Cohen E. L. and Wurtman R. J. (1976) Brain acetylcholine: control by dietary choline. *Science* **191**, 561–562.

Collier B. and Ilson D. (1977) The effects of preganglionic nerve stimulation on the accumulation of certain analogues of choline by a sympathetic ganglion. *J. Physiol.* **264**, 489–509.

Collier B. and Katz H. S. (1974) Acetylcholine synthesis from recaptured choline by a sympathetic ganglion. *J. Physiol.* **238**, 639–655.

Daws L. C., Toney G. M., Davis D. J., Gerhardt G. A. and Frazer A. (1997) In vivo chronoamperometric measurements of the clearance of exogenously applied serotonin in the rat dentate gyrus. *J. Neurosci. Meth.* **78**, 139–150.

Everitt B. J. and Robbins T. W. (1997) Central cholinergic systems and cognition. *Ann. Rev. Psychol.* **48**, 649–684.

Farber S. A., Savci V., Wei A., Slack B. E. and Wurtman R. J. (1996) Choline's phosphorylation in rat striatal slices is regulated by the activity of cholinergic neurons. *Brain Res.* **723**, 90–99.

Ferguson S. M. and Blakely R. D. (2004) The choline transporter resurfaces: new roles for synaptic vesicles? *Mol. Intervent.* **4**, 22–37.

Ferguson S. M., Savchenko V., Apparsundaram S., Zwick M., Wright J., Heilman C. J., Yi H., Levey A. I. and Blakely R. D. (2003) Vesicular localization and activity-dependent trafficking of presynaptic choline transporters. *J. Neurosci.* **23**, 9697–9709.

Ferguson S. M., Bazalakova M., Savchenko V., Tapia J. C., Wright J. and Blakely R. D. (2004) Lethal impairment of cholinergic neurotransmission in hemicholinium-3-sensitive choline transporter knockout mice. *Proc. Natl. Acad. Sci. USA* **101**, 8762–8767.

Freeman J. J., Macri J. R., Choi R. L. and Jenden D. J. (1979) Studies on the behavioral and biochemical effects of hemicholinium *in vivo*. *J. Pharmacol. Exp. Ther.* **210**, 91–97.

Friedemann M. N. and Gerhardt G. A. (1992) Regional effects of aging on dopaminergic function in the Fischer-344 rat. *Neurobiol. Aging* **13**, 325–332.

Gates J. Jr, Ferguson S. M., Blakely R. D. and Apparsundaram S. (2004) Regulation of Choline Transporter Surface Expression and Phosphorylation by Protein Kinase C and Protein Phosphatase 1/2A. *J. Pharmacol. Exp. Ther.* **310**, 536–545.

Giros B., Jaber M., Jones S. R., Wightman R. M. and Caron M. G. (1996) Hyperlocomotion and indifference to cocaine and amphetamine in mice lacking the dopamine transporter. *Nature* **379**, 606–612.

Greenwald A. G., Gonzalez R., Harris R. J. and Guthrie D. (1996) Effect sizes and, p. values: what should be reported and what should be replicated? *Psychophysiology* **33**, 175–183.

Growdon J. H., Cohen E. L. and Wurtman R. J. (1977) Treatment of brain disease with dietary precursors of neurotransmitters. *Ann. Intern. Med.* **86**, 337–339.

Guyenet P., Lefresne P., Rossier J., Beaujouan J. C. and Glowinski J. (1973) Effect of sodium, hemicholinium-3 and antiparkinson drugs on (14C) acetylcholine synthesis and (3H) choline uptake in rat striatal synaptosomes. *Brain Res.* **62**, 523–529.

Haga T. (1971) Synthesis and release of (14 C) acetylcholine in synaptosomes. *J. Neurochem.* **18**, 781–798.

Hasselmo M. E. and McGaughy J. (2004) High acetylcholine levels set circuit dynamics for attention and encoding and low acetylcholine levels set dynamics for consolidation. *Progr. Brain Res.* **145**, 201–231.

Herzog C. D., Nowak K. A., Sarter M. and Bruno J. P. (2003) Microdialysis without acetylcholinesterase inhibition reveals an age-related attenuation in stimulated cortical acetylcholine release. *Neurobiol. Aging* **24**, 861–863.

Holley L. A., Wiley R. G., Lappi D. A. and Sarter M. (1994) Cortical cholinergic deafferentation following the intracortical infusion of 192 IgG-saporin: a quantitative histochemical study. *Brain Res.* **663**, 277–286.

Ikarashi Y., Takahashi A., Ishimaru H., Arai T. and Maruyama Y. (1997) Relations between the extracellular concentrations of choline and acetylcholine in rat striatum. *J. Neurochem.* **69**, 1246–1251.

Kessler P. D. and Marchbanks R. M. (1979) Choline transport is not coupled to acetylcholine synthesis. *Nature* **279**, 542–544.

Klein J., Koppen A. and Loffelholz K. (1998) Regulation of free choline in rat brain: dietary and pharmacological manipulations. *Neurochem. Int.* **32**, 479–485.

Klein J., Weichel O., Ruhr J., Dvorak C. and Loffelholz K. (2002) A homeostatic mechanism counteracting K (+)-evoked choline release in adult brain. *J. Neurochem.* **80**, 843–849.

Koppen A., Klein J., Schmidt B. H., van der Staay F. J. and Loffelholz K. (1996) Effects of nicotinamide on central cholinergic transmission and on spatial learning in rats. *Pharmacol. Biochem. Behav.* **53**, 783–790.

Koppen A., Klein J., Erb C. and Loffelholz K. (1997) Acetylcholine release and choline availability in rat hippocampus: effects of exogenous choline and nicotinamide. *J. Pharmacol. Exp. Ther.* **282**, 1139–1145.

Koshimura K., Miwa S., Lee K., Hayashi Y., Hasegawa H., Hamahata K., Fujiwara M., Kimura M. and Itokawa Y. (1990) Effects of choline administration on in vivo release and biosynthesis of acetylcholine in the rat striatum as studied by in vivo brain microdialysis. *J. Neurochem.* **54**, 533–539.

Kus L., Borys E., Ping Chu Y., Ferguson S. M., Blakely R. D., Emborg M. E., Kordower J. H., Levey A. I. and Mufson E. J. (2003) Distribution of high affinity choline transporter immunoreactivity in the primate central nervous system. *J. Comp. Neurol.* **463**, 341–357.

Lockman P. R. and Allen D. D. (2002) The transport of choline. *Drug. Dev. Ind. Pharm.* **28**, 749–771.

Manaker S., Wieczorek C. M. and Rainbow T. C. (1986) Identification of sodium-dependent, high-affinity choline uptake sites in rat brain with [3H]hemicholinium-3. *J. Neurochem.* **46**, 483–488.

Marshall D. L. and Wurtman R. J. (1993) Effect of choline on basal and stimulated acetylcholine release: an in vivo microdialysis study using a low neostigmine concentration. *Brain Res.* **629**, 269–274.

McGaughy J., Kaiser T. and Sarter M. (1996) Behavioral vigilance following infusions of 192 IgG-saporin into the basal forebrain: selectivity of the behavioral impairment and relation to cortical AChE-positive fiber density. *Behav. Neurosci.* **110**, 247–265.

Mesulam M. (2004) The cholinergic lesion of Alzheimer's disease: pivotal factor or side show? *Learn. Mem.* **11**, 43–49.

Misawa H., Nakata K., Matsuura J., Nagao M., Okuda T. and Haga T. (2001) Distribution of the high-affinity choline transporter in the central nervous system of the rat. *Neuroscience* **105**, 87–98.

Nicholson C. (1985) Diffusion from an injected Volume of a substance in brain tissue with arbitrary Volume fraction and tortuosity. *Brain Res.* **333**, 325–329.

Parikh V., Pomerleau F., Huettl P., Gerhardt G. A., Sarter M. and Bruno J. P. (2004) Rapid assessment of in vivo cholinergic transmission by amperometric detection of changes in extracellular choline levels. *Eur. J. Neurosci.* **20**, 1545–1554.

Paxinos G. and Watson C. (1988) *The Rat Brain in Stereotaxic Coordinates.*, 4th edn. Academic Press, San Diego.

Pizzo D. P., Waite J. J., Thal L. J. and Winkler J. (1999) Intraparenchymal infusions of 192 IgG-saporin: development of a method for selective and discrete lesioning of cholinergic basal forebrain nuclei. *J. Neurosci. Meth.* **91**, 9–19.

Rousseau S. J., Jones I. W., Pullar I. A. and Wonnacott S. (2005) Presynaptic alpha7 and non-alpha7 nicotinic acetylcholine receptors modulate [3H]d-aspartate release from rat frontal cortex in vitro. *Neuropharmacology* **49**, 59–72.

Saltarelli M. D., Lowenstein P. R. and Coyle J. T. (1987) Rapid in vitro modulation of [3H]hemicholinium-3 binding sites in rat striatal slices. *Eur. J. Pharmacol.* **135**, 35–40.

Saltarelli M. D., Yamada K. and Coyle J. T. (1990) Phospholipase A_2 and ^{3}H-hemicholinium-3 binding sites in rat brain: a potential second-messenger role for fatty acids in the regulation of high-affinity choline uptake. *J. Neurosci.* **10**, 62–72.

Sarter M. and Parikh V. (2005) Choline transporters, cholinergic transmission and cognition. *Nat. Rev. Neurosci.* **6**, 48–56.

Sarter M., Hasselmo M. E., Bruno J. P. and Givens B. (2005a) Unraveling the attentional functions of cortical cholinergic inputs: interactions between signal-driven and top-down cholinergic modulation of signal detection. *Brain Res. Rev.* **48**, 98–111.

Sarter M., Nelson C. L. and Bruno J. P. (2005b) Cortical cholinergic transmission and cortical information processing following psychostimulant-sensitization: implications for models of schizophrenia. *Schizophren. Bull.* **31**, 117–138.

Simon J. R. and Kuhar M. G. (1975) Impulse-flow regulation of high affinity choline uptake in brain cholinergic nerve terminals. *Nature* **255**, 162–163.

Simon J. R. and Kuhar M. G. (1976) High affinity choline uptake: ionic and energy requirements. *J. Neurochem.* **27**, 93–99.

Simon J. R., Atweh S. and Kuhar M. J. (1976) Sodium-dependent high affinity choline uptake: a regulatory step in the synthesis of acetylcholine. *J. Neurochem.* **26**, 909–922.

Slotkin T. A., Nemeroff C. B., Bissette G. and Seidler F. J. (1994) Overexpression of the high affinity choline transporter in cortical regions affected by Alzheimer's disease. Evidence from rapid autopsy studies. *J. Clin. Invest.* **94**, 696–702.

Tago H., Kimura H. and Maeda T. (1986) Visualization of detailed acetylcholinesterase fiber and neuron staining in rat brain by a sensitive histochemical procedure. *J. Histochem. Cytochem.* **34**, 1431–1438.

Ulus I. H., Millington W. R., Buyukuysal R. L. and Kiran B. K. (1988) Choline as an agonist: determination of its agonistic potency on cholinergic receptors. *Biochem. Pharmacol.* **37**, 2747–2755.

Ulus I. H., Wurtman R. J., Mauron C. and Blusztajn J. K. (1989) Choline increases acetylcholine release and protects against the stimulation-induced decrease in phosphatide levels within membranes of rat corpus striatum. *Brain Res.* **484**, 217–227.

Vinson P. N. and Justice J. B. Jr (1997) Effect of neostigmine on concentration and extraction fraction of acetylcholine using quantitative microdialysis. *J. Neurosci. Meth* **73**, 61–67.

Waite J. J., Wardlow M. L., Chen A. C., Lappi D. A., Wiley R. G. and Thal L. J. (1994) Time course of cholinergic and monoaminergic changes in rat brain after immunolesioning with 192 IgG-saporin. *Neurosci. Lett.* **169**, 154–158.

Wightman R. M., Amatore C., Engstrom R. C., Hale P. D., Kristensen E. W., Kuhr W. G. and May L. J. (1988) Real-time characterization of dopamine overflow and uptake in the rat striatum. *Neuroscience* **25**, 513–523.

Wiley R. G., Oeltmann T. N. and Lappi D. A. (1991) Immunolesioning: selective destruction of neurons using immunotoxin to rat NGF receptor. *Brain Res.* **562**, 149–153.

Wurtman R. J. (1992) Choline metabolism as a basis for the selective vulnerability of cholinergic neurons. *Trends Neurosci.* **15**, 117–122.

Yamamura H. I. and Snyder S. H. (1972) Choline: high-affinity uptake by rat brain synaptosomes. *Science* **178**, 626–628.

Zaborszky L. (2002) The modular organization of brain systems. Basal forebrain: the last frontier. *Prog. Brain Res.* **136**, 359–372.

Zahniser N. R. and Doolen S. (2001) Chronic and acute regulation of Na+/Cl–dependent neurotransmitter transporters: drugs, substrates, presynaptic receptors, and signaling systems. *Pharmacol. Ther.* **92**, 21–55.

Zahniser N. R. and Sorkin A. (2004) Rapid regulation of the dopamine transporter: role in stimulant addiction? *Neuropharmacology* **47**, 80–91.

Zahniser N. R., Larson G. A. and Gerhardt G. A. (1999) In vivo dopamine clearance rate in rat striatum: regulation by extracellular dopamine concentration and dopamine transporter inhibitors. *J. Pharmacol. Exp. Ther.* **289**, 266–277.

Zapata A., Capdevila J. L. and Trullas R. (2000) Role of high-affinity choline uptake on extracellular choline and acetylcholine evoked by NMDA. *Synapse* **35**, 272–280.

